

# FILMS based ANC System – Evaluation and Practical Implementation

Branislav Vuksanović, and Dragana Nikolić

**Abstract**—This paper describes the implementation and testing of a multichannel active noise control system (ANCS) based on the filtered-inverse LMS (FILMS) algorithm. The FILMS algorithm is derived from the well-known filtered-x LMS (FXLMS) algorithm with the aim to improve the rate of convergence of the multichannel FXLMS algorithm and to reduce its computational load. Laboratory setup and techniques used to implement this system efficiently are described in this paper. Experiments performed in order to test the performance of the FILMS algorithm are discussed and the obtained results presented.

**Keywords**—Active noise control, adaptive filters, inverse filters, LMS algorithm, FILMS algorithm.

## I. INTRODUCTION

THIS paper describes the implementation and testing of a multichannel active noise control system (ANCS) based on the filtered-inverse LMS (FILMS) algorithm. The FILMS algorithm is derived from the well-known filtered-x LMS (FXLMS) algorithm with the aim to improve the rate of convergence of the multichannel FXLMS algorithm and to reduce its computational load. Laboratory setup and techniques used to implement this system efficiently are described in this paper. Experiments performed in order to test the performance of the FILMS algorithm are discussed and the obtained results presented.

## II. AN OVERVIEW OF MFILMS ALGORITHMS

A block scheme of the single-reference/multiple-output FILMS-based ANCS is shown in Fig. 1. Pre-equaliser – inverse matrix, denoted as  $\mathbf{H}$ , consists of the  $K \times M$  estimates of the secondary paths inverse filters  $h_{km}$  measured between the  $K$  secondary loudspeakers and the  $M$  error microphones each of length  $L_h$ . This pre-equaliser block is placed in series with an adaptive filter block  $\mathbf{W}$  and its task is to neutralise the influence of the secondary electroacoustic paths  $\mathbf{S}$ , each of length  $L_s$ , which distort the set of cancelling signals  $y_i$ . The combination of the delayed inverse plant model and the real plant is approximately a pure delay with the uniform frequency response, thus eliminating the eigenvalue spread caused by the direct plant (set of secondary acoustic paths

B. Vuksanović is with the University of Portsmouth, Department of Electronic and Electrical Engineering, Portsmouth, Hampshire, UK. (phone: 9944-2392-842159; e-mail: branislav.vuksanovic@port.ac.uk).

D. Nikolić is with the Institute of Sound and Vibration Research, University of Southampton, UK.

represented by block  $\mathbf{S}$  in Fig. 1). Update filter block matrix  $\Delta$  consists of  $M \times M$  update filters whose coefficients depend on the chosen adaptive update technique applied in the filtering branches.

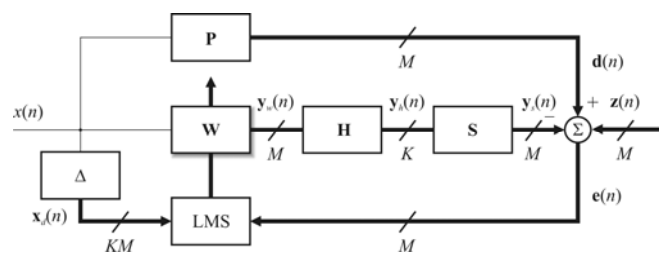


Fig. 1 Multichannel realisation of the FILMS algorithm

Complete Multichannel FILMS (CMFILMS) algorithm is a multichannel FILMS algorithm that uses signals from all  $M$  error microphones for the adjustment of the coefficients of all  $M$  adaptive filters. This algorithm is robust, but its computational requirement grows rapidly with the number of channels implemented. The complexity of the CMFILMS algorithm however, can be significantly reduced if only one term of the update equation, corresponding to one error signal, is used to update all filter coefficients during each sampling interval. This approach allows for a more efficient realisation of the MFILMS algorithm since the matching combinations of the secondary plant impulse responses and its inverses can be replaced with pure delays. This modification of the CMFILMS algorithm is referred to as Complete Single-Error Multichannel FILMS (CSEMFILMS) algorithm.

A considerable computational savings of the CMFILMS algorithm could also be achieved by suppressing cross-cancellation in the inverse plant. This setup is restricted to the multichannel ANCS with the same number of loudspeakers and error microphones. This variant of the CMFILMS is denoted here as Simplified MFILMS (SMFILMS) algorithm and its single-error version as SSEMFILMS. The set of equations used to describe the MFILMS algorithm is given in Table I according to the notation from Fig. 1.

Equation (6) represents the general adaptive update equation for the MFILMS algorithm where  $\mathbf{X}_{st}$  matrix corresponds to the result of filtering the reference signal through the  $M \times M$  update filter block matrix  $\Delta$  shown in Fig. 1. This filter matrix depends on the inverse structure and the secondary plant that follows the adaptive filters and is different for all four ver-

sions of the MFILMS algorithm. The filters  $\Delta_{m'm}$  from the update matrix  $\Delta$  ( $m=1, M, m'=1, M$ ), are given with (7).

TABLE I  
 SUMMARY OF THE MFILMS ALGORITHM EQUATIONS

$\mathbf{d}(n) = \mathbf{P}^T \mathbf{x}'(n)$	(1)
$\mathbf{y}_w(n) = \mathbf{X}^T(n) \mathbf{W}(n)$	(2)
$\mathbf{y}_h(n) = \mathbf{H} * \mathbf{y}_w(n)$	(3)
$\mathbf{y}_s(n) = (\mathbf{S} * \mathbf{H}) * \mathbf{y}_w(n)$	(4)
$\mathbf{e}(n) = \mathbf{d}(n) - \mathbf{y}_s(n) + \mathbf{z}(n)$	(5)
$\mathbf{W}(n+1) = \mathbf{W}(n) + \mu \mathbf{X}_{sh} \mathbf{e}(n)$	(6)
$\Delta_{m'm} = \begin{cases} \sum_{k=1}^K \hat{\mathbf{s}}_{km} * \hat{\mathbf{h}}_{km} & \text{CMFILMS} \\ \begin{cases} \sum_{k=1}^K \delta(n - D_{km}) & \text{if } m' = m \\ 0 & \text{otherwise} \end{cases} & \text{CSEMFILMS} \\ \hat{\mathbf{s}}_{m'm} * \hat{\mathbf{h}}_{m'm} & \text{SMFILMS} \\ \begin{cases} \delta(n - D_{mm}) & \text{if } m' = m \\ 0 & \text{otherwise} \end{cases} & \text{SSEMFILMS} \end{cases} \quad (7)$	

For the CMFILMS and SMFILMS versions of the algorithm those filters must be long enough to adequately represent the result of convolution  $\hat{\mathbf{s}} * \hat{\mathbf{h}}$ , and for the single-error approach they are determined by the maximum delay in the multichannel secondary plant,  $D_{km}$ .

The estimation of computational requirements of each of the proposed MFILMS algorithms is based on the number of multiplications during one algorithm iteration. Those estimates are given in TABLE along with the similar data for the multichannel FXLMS (MFXLMS) algorithm. The requirements for the single-error versions of both CMFILMS and SMFILMS algorithms are reduced by  $M^2(L_w + L_s + L_h - 1) - ML_w$  multiplications. The use of delay lines in filtering branches makes CSEMFILMS and SSEMFILMS algorithms far less computational and memory demanding than their full-update versions, CMFILMS and SMFILMS.

TABLE II  
 COMPUTATIONAL COMPLEXITY OF THE PROPOSED MULTICHANNEL ALGORITHMS

Algorithms	Number of multiplies
MFXLMS	$KML_s + K(M+1)L_w + M$
CMFILMS	$KML_n + M^2(L_w + L_s + L_h - 1) + ML_w + M$
CSEMFILMS	$KML_n + 2ML_w + M$
SMFILMS	$ML_n + M^2(L_w + L_s + L_h - 1) + ML_w + M$
SSEMFILMS	$ML_n + 2ML_w + M$

The number of required computations for the various number of channels implemented in the system, is calculated according to Table II and plotted in Fig. 2 for all four versions of the MFILMS. It can be seen that the complexity of the SMFILMS is comparable to the CMFILMS ones for the lower number of channels but SMFILMS becomes more efficient for the number of channels greater than 8.

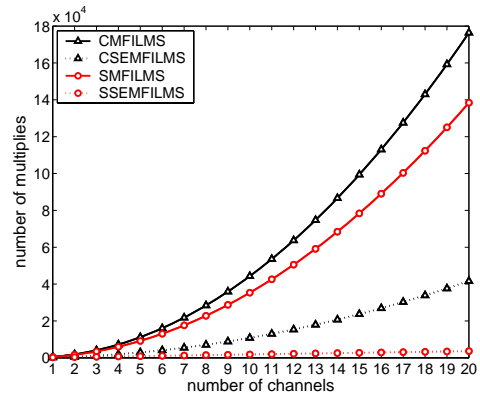


Fig. 2 Computational complexity of the MFILMS for various number of system channels and filter lengths  $L_s=200$ ,  $L_h=100$  and  $L_w=40$

### III. LABORATORY SETUP AND SOFTWARE DESIGN ISSUES

A schematic of the equipment used to implement the prototype ANCS is shown in Fig. 3. Data acquisition and signal processing in the multichannel ANCS are performed using the Analog Devices SHARC processor ADSP21161N.

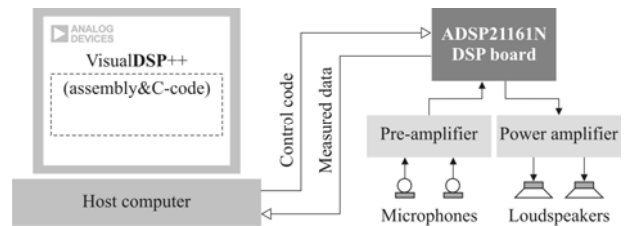


Fig. 3 Hardware used for ANC experiment

This is a 32-bit floating-point DSP processor with a 100 MHz core clock. The audio interface on the 21161N EZ-KIT Lite board used in the experiments is realised through the AD1836 multichannel codec with six DACs and four ADCs limiting the maximum number of control channels implemented in the laboratory to three. Additional daughter card based around the same AD1836 codec is available on the market and could be used to extend the number of channels available on the system.

Since the operating range of ANC is 150 Hz-2 kHz, the sampling rate selected for this application is  $f_s=4$  kHz resulting in the sampling time  $T_s=0.25$  ms. The number of instructions required for the implementation of the multichannel FXLMS and FILMS algorithms increases with the increase in the filter length which calls for the highly optimised code to satisfy the real-time constraint of 0.25 ms computation time. It is important to note that the electrical delay from the reference input to the loudspeaker should be less than the acoustic delay, i.e. the computation time for the “anti-noise” should be small fraction of the sampling interval.

To reduce the computational burden, all ANC programs written for the laboratory experiments had to be further analysed and modified in order to find the bottlenecks and to im-

prove the execution time. Elimination of even one cycle from a loop that executes hundreds of times can significantly improve the algorithm execution time. It is also important to be aware of the trade-offs between the various performance parameters such as throughput (execution speed), memory usage, I/O bandwidth and computation power dissipation. Optimising an application for speed often means a corresponding decrease in computation power consumption, but an increase in memory usage. Optimising for memory usage on the other hand, may also result in a decrease in power consumption due to a fewer memory accesses, but an offsetting decrease in code performance.

#### IV. INVERSE SYSTEM ESTIMATION

In order to implement both the multichannel FXLMS as well as FILMS-based systems, it is necessary to estimate a response of a complete system plant consisting of all secondary paths in the system. Adaptive system identification technique described in [1] based on the LMS update of the adaptive filter is usually used to accomplish this task.

In addition to direct plant estimation, the FILMS-based ANCS also requires the estimation of the inverted versions of the measured secondary path responses. The inversion of the system transfer function is the key point of the equalising procedure in many DSP applications, and a number of advanced techniques were developed to this aim [4]-[7]. However, almost all of those techniques produce a large number of FIR filter coefficients, and thus cannot be implemented in a real-time on a low-cost DSP.

The perfect equalisation filter is the inverse filter, which equalises not only the magnitude but also the phase of the system frequency response. However, there are difficulties in obtaining estimates of inverse plant functions, as inverted functions are potentially unstable [8]. For example, proper functions (functions with more poles than zeros) become improper functions having more zeros than poles when inverted. Or even more seriously, functions with "unstable" zeros lying outside of the unit circle in the z-domain become unstable poles (non-minimum phase functions) with large (advanced) responses lying to the left of time zero, when inverted. Zeros lying inside the unit circle have exponentially decreasing positive time (delayed) sequences to the right of time zero, after inversion. Zeros lying on the unit circle have both positive and negative time sequences. Zeros lying near to the centre of the unit circle or at large distances outside the unit circle have a weak influence on the system, resulting in short time sequences. Functions having large exponentially decaying negative time (advanced) sequences to the left of time zero cannot be realised. Thus, a delay is required to move these functions to the right of time zero forcing the functions from advanced (future) into delayed (past), in this upside down world of time [8].

In the conventional least squares (LS) approach, an approximated solution of the form  $\mathbf{C}_s \mathbf{h} = \Delta$  for the inverse filter coefficient vector  $\mathbf{h}$ , can be computed as [5]:

$$\mathbf{h} = (\mathbf{C}_s^T \mathbf{C}_s)^{-1} \mathbf{C}_s^T \Delta \quad (8)$$

where  $\mathbf{C}_s$  represents the  $(L_s+L_h-1) \times L_h$  convolution matrix of the system impulse responses of length  $L_s$  given by:

$$\mathbf{C}_s = \begin{bmatrix} \mathbf{s} & & & \mathbf{0} \\ & \mathbf{s} & & \\ & & \ddots & \\ \mathbf{0} & & & \mathbf{s} \end{bmatrix} = \begin{bmatrix} s_0 & & & \mathbf{0} \\ s_1 & s_0 & & \\ \vdots & s_1 & \ddots & s_0 \\ s_{L_s-1} & \vdots & \ddots & s_1 \\ & s_{L_s-1} & & \vdots \\ \mathbf{0} & & \ddots & s_{L_s-1} \end{bmatrix} \quad (9)$$

and  $\Delta$  is the column vector of length  $L_s+L_h-1$ , with coefficients defined as:

$$\Delta_k = \begin{cases} 1 & k = D+1 \\ 0 & \text{otherwise} \end{cases}, \quad k=1, L_s+L_h-1 \quad (10)$$

This unique pseudo-inverse matrix is also known as Moore-Penrose generalised matrix inverse [9]. Since, the calculation of the inverse of large square matrix  $\mathbf{C}_s^T \mathbf{C}_s$  of the order  $L_s+L_h-1$  is a very complicated and extremely time consuming operation, a direct implementation of the proposed structure would require a computational cost far too high to be implemented on a low-cost DSP. Furthermore, due to accumulation of truncation and rounding-off errors the result can become worthless. An accurate inverse response estimate of the secondary plant can be obtained using the LMS adaptive algorithm described in the following subsections. Moreover, this algorithm converges to the optimal (Wiener) solution [10] defined by (8).

##### A. Single-Channel Adaptive Inverse System Estimation

Fig. 4 is showing the system setup for the estimation of the secondary path inverse in the single-channel configuration. Adaptive filter  $W(z)$ , whilst driving the error between its output  $y_w(n)$  and delayed input signal  $d(n)$  to zero is forming the inverse model of the secondary path  $S(z)$  between the loudspeaker and the error microphone. Delay  $D$ , used in order to obtain a stable non-causal inverse filter, needs to be large enough to account for the propagation delay of the secondary path  $S(z)$ ,  $D_s$ , and the adaptive (inverse) filter  $W(z)$ ,  $D_h$ , i.e.  $D \geq D_s + D_h$ . If delay  $D$  is smaller than the overall delay  $D_s + D_h$ , system will be unstable and the algorithm would diverge rather than converge. Providing a suitable choice of delay  $D$  and the length of the adaptive filter  $L_w$ , a good delayed inverse of the secondary path can be estimated using this setup [8], [11].

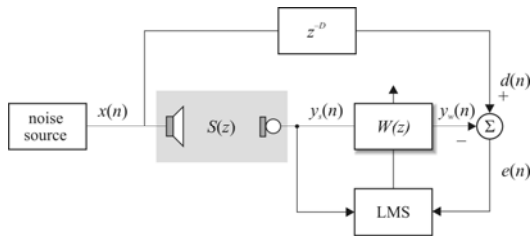


Fig. 4 Block diagram of direct single-channel inverse estimation

**B. Multichannel Adaptive Inverse System Estimation**

The LMS-based approach can also be used to find all the inverse filters for the  $K \times M$  channel ANCS in situ, in order to incorporate those filters in the proposed MFILMS algorithms. Two potential schemes for the estimation of the multichannel inverse plant have been implemented and tested.

The two-channel pre-equaliser structure combined with cross-cancellation technique proposed by Nelson [12] estimates four inverse filters that can be employed in CMFILMS algorithm. This scheme is shown in Fig. 5(a). Another approach is to use the two-channel setup based on the FXLMS configuration in order to estimate only two equalising filters that can be used in SMFILMS algorithm. The influence of both direct and cross paths is included and accounted for in those adaptive filters. This scheme is shown in Fig. 5(b).

**V. SYSTEM IMPLEMENTATION**

Two- and three-channel FXLMS, CSEMFILMS and SSEMFILMS algorithms are implemented in laboratory and the results of those experiments are presented in this section. Direct and inverse single channel estimation approaches described in the previous section were used to obtain the impulse responses of the secondary paths and their inverses for the use in FXLMS and FILMS algorithms. The lengths of the impulse and inverse responses are  $L_s=200$  and  $L_i=100$  taps. The responses of first 3 (out of 9) cancelling paths and their inverses in the three-channel ANCS setup in the laboratory are presented in Fig. 6 and Fig. 7.

Error signals and learning curves for two-channel FXLMS, CSEMFILMS and SSEMFILMS algorithms can be observed on the Fig. 8. Faster convergence of two tested variants of the FILMS algorithm, compared to FXLMS algorithm can be clearly identified on this figure where the signal measured at the error microphone 2 from the system is plotted in time domain. The CSEMFILMS algorithm reaches its steady state after approximately 5000 iterations (1.25 s), SSEMFILMS after 15000 iterations (3.75 s) and FXLMS after 25000 iterations (6.25 s).

To assess the steady state performance of those algorithms and the level of residual signal on the error microphones, the error signal measured before and after cancellation for the three-channel ANCS is plotted in Fig. 9 in both time and frequency domains. In addition to the higher convergence rate compared to that of the FXLMS algorithm, two implemented variants of FILMS algorithm can also achieve lower error

levels at the microphones after the convergence phase. The two higher frequencies in the primary signal (500 Hz and 600 Hz) are not cancelled using the FXLMS. Increasing the number of adaptive filter taps in the FXLMS configuration to  $L_w=100$  taps, did not improve its performance, resulting only in a further deterioration of the convergence rate. The CSEMFILMS, for both configurations (two- and three-channel), completely cancelled all five frequencies in the primary signal at the measurement position of the second error microphone. The similar performance is achieved for even smaller number of filter taps ( $L_w=40$  and 60) used in this algorithm. In order to compare the convergence rate of those algorithms, the same number of adaptive filter taps is used for each algorithm to ensure that the convergence is not affected by this parameter. Although the SSEMFILMS algorithm results in the similar levels of attenuation per each frequency as the FXLMS, it is much less computationally demanding and faster than FXLMS.

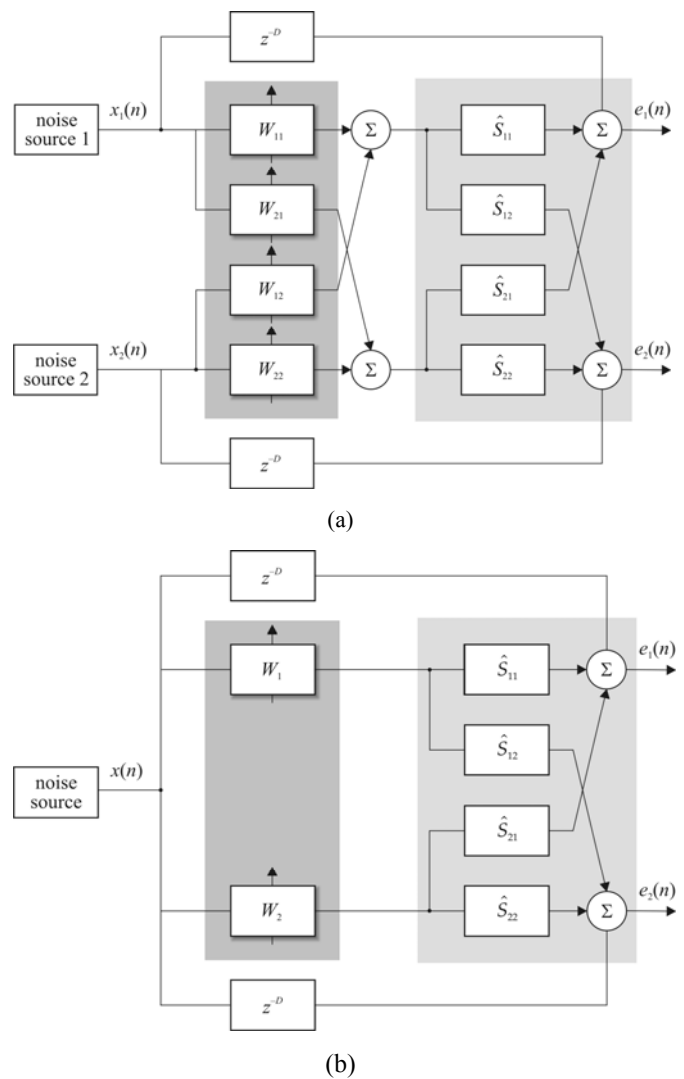


Fig. 5 Block diagram of the two-channel indirect inverse secondary path estimation (a) scheme with four inverse filters (b) scheme with two inverse filters

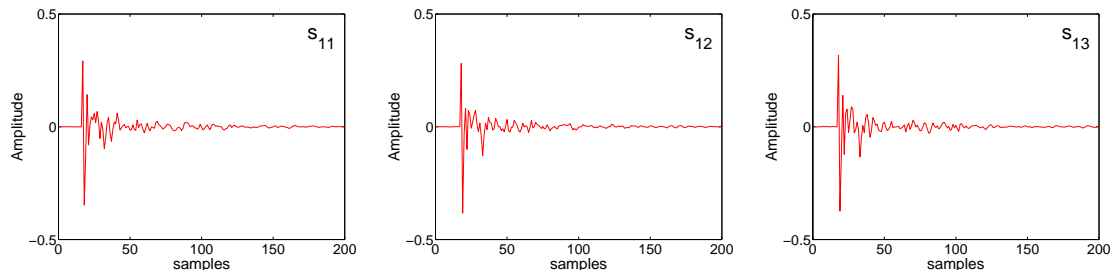


Fig. 6 Estimated secondary path impulse responses between first loudspeaker and three error microphones in the three-channel ANCS

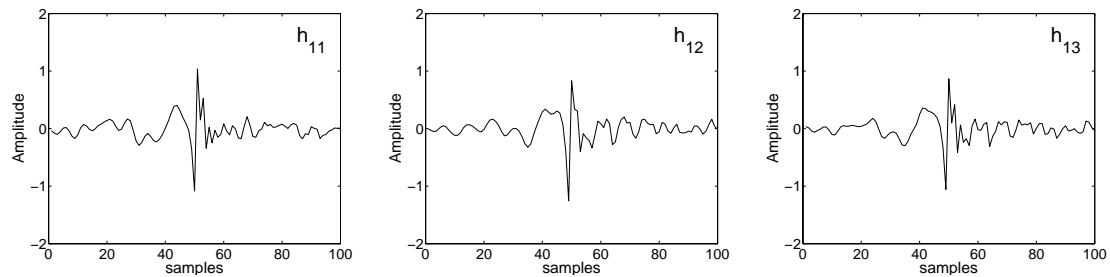


Fig. 7 Estimated inverse filter responses of the secondary paths between first loudspeaker and three error microphones in the three-channel ANCS from Fig. 6

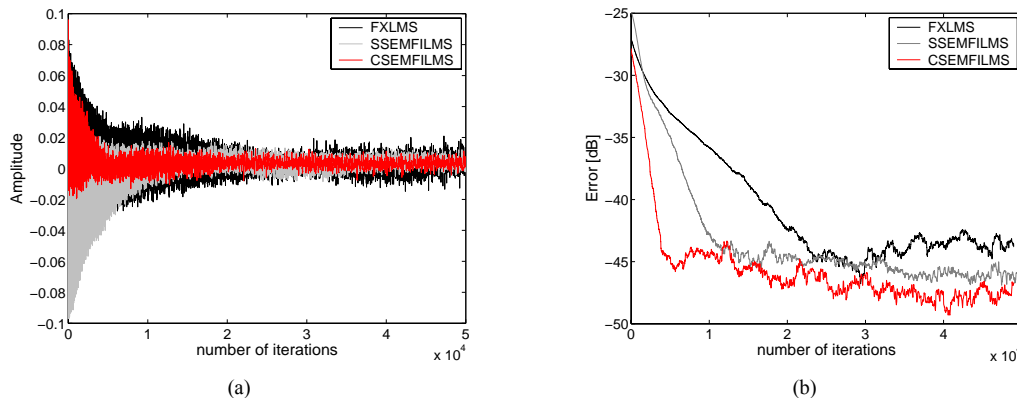


Fig. 8 Comparison of the two-channel FXLMS, CSEMFILMS and SSEMFILMS algorithms; (a) time evolution of the error signal and (b) learning curves

To assess the steady state performance of those algorithms and the level of residual signal on the error microphones, the error signal measured before and after cancellation for the three-channel ANCS is plotted in Fig. 9 in both time and frequency domains. In addition to the higher convergence rate compared to that of the FXLMS algorithm, two implemented variants of FILMS algorithm can also achieve lower error levels at the microphones after the convergence phase. The two higher frequencies in the primary signal (500 Hz and 600 Hz) are not cancelled using the FXLMS. Increasing the number of adaptive filter taps in the FXLMS configuration to  $L_w=100$  taps, did not improve its performance, resulting only in a further deterioration of the convergence rate. The

CSEMFILMS, for both configurations (two- and three-channel), completely cancelled all five frequencies in the primary signal at the measurement position of the second error microphone. The similar performance is achieved for even smaller number of filter taps ( $L_w=40$  and  $60$ ) used in this algorithm. In order to compare the convergence rate of those algorithms, the same number of adaptive filter taps is used for each algorithm to ensure that the convergence is not affected by this parameter. Although the SSEMFILMS algorithm results in the similar levels of attenuation per each frequency as the FXLMS, it is much less computationally demanding and faster than FXLMS.

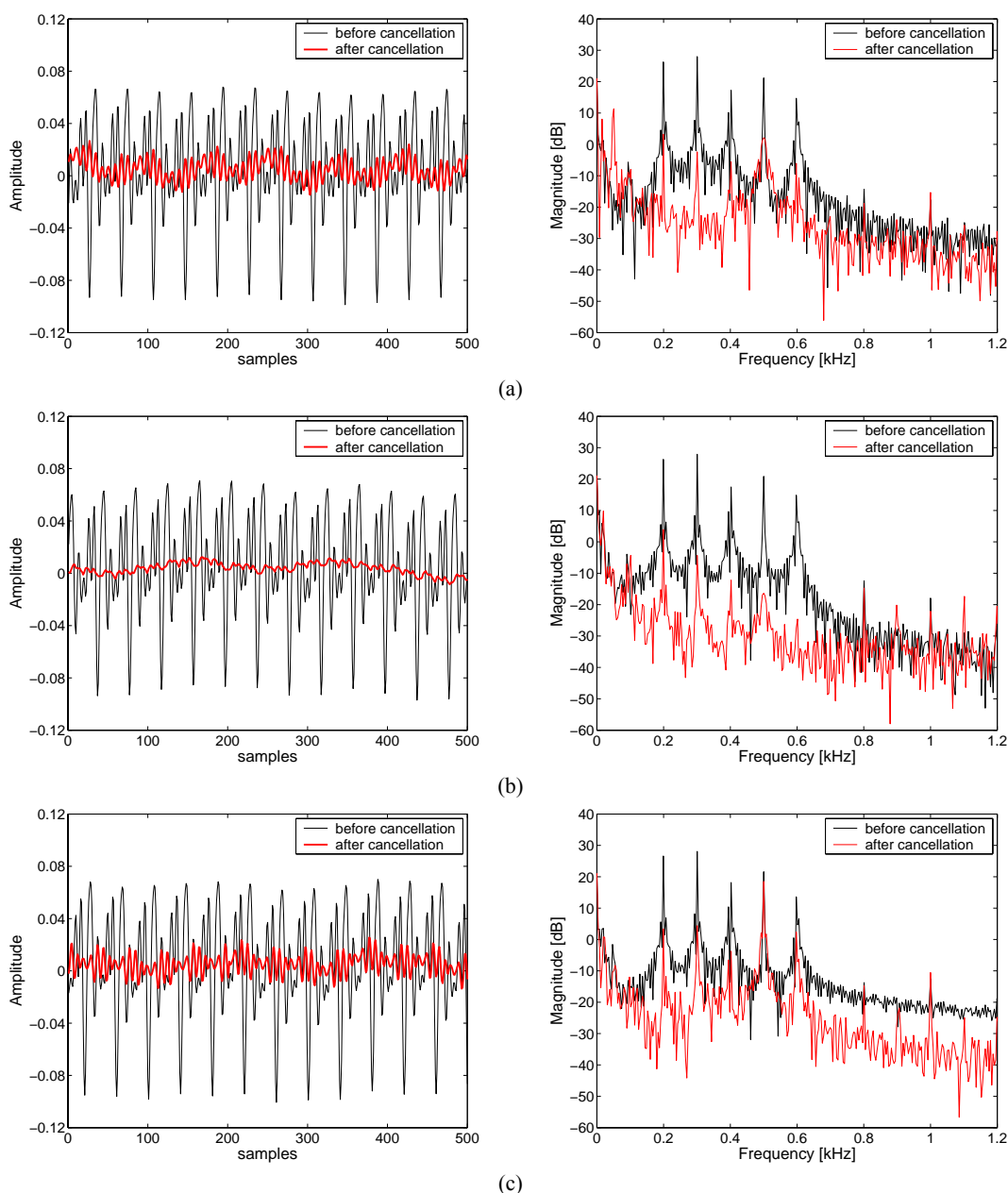


Fig. 9 Error signal before and after cancellation in time (left) and frequency (right) domain for the three-channel (a) FXLMS, (b) CSEMFILMS and (c) SSEMFILMS algorithms

## VI. SUMMARY AND CONCLUSION

Multichannel FILMS as well as FXLMS based ANCSs are designed and implemented in laboratory using the Analog Devices ADSP 21161N EZ-Kit Lite. Major concerns related to real-time constraints of the ANCS are considered and discussed in this paper. Difficulties in obtaining accurate estimates of inverse plant functions have been considered and both single-channel and multichannel adaptive inverse system estimation techniques implemented and tested.

Finally, the properties of the FILMS algorithm based ANCS have been established and demonstrated using both single and multiple control channel configurations. The con

vergence rate of the FILMS algorithm is found to be comparable with the well-known FXLMS algorithm and the computational load is reduced providing good estimates of secondary plant and its inverse can be obtained. Various multichannel FILMS configuration are implemented and tested. Stability, speed of convergence, steady state performance and computational requirements for each approach are measured.

## REFERENCES

- [1] S. M. Kuo and D. R. Morgan, Active noise control systems: algorithms and DSP implementations. New York: John Wiley&Sons, 1996.
- [2] B. Vuksanović and D. Nikolić, "Behaviour of the FILMS algorithm," in ACTIVE 2006. Adelaide, Australia, 2006.

- [3] D. Nikolić and B. Vuksanović, "Multichannel filtered-inverse least mean square algorithms – development and analysis," in 2007 IEEE International Workshop on Machine Learning for Signal Processing, Thessaloniki, Greece, 2007.
- [4] S. T. Neely and J. B. Allen, "Invertibility of a room impulse response," *Journal of the Acoustic Society of America*, vol. 66, pp. 165-169, 1979.
- [5] M. Miyoshi and Y. Kaneda, "Inverse filtering of room acoustics," *IEEE Transactions on Acoustic, Speech and Audio Processing*, vol. 36, pp. 145-152, 1988.
- [6] A. Farina, E. Ugolotti, A. Bellini, G. Cibelli, and C. Morandi, "Inverse numerical filters for linearization of loudspeaker's response," presented at DAFX-98 Conference, Barcelona, Spain, 1998.
- [7] J. Jan, *Digital signal filtering, analysis and restoration*. London: IEE Press, 2000.
- [8] S. E. Wright, H. Atmoko, and B. Vuksanovic, "Active control of environmental noise, VIII: increasing the response to primary source changes including unpredictable noise," *Journal of Sound and Vibration*, vol. 274, pp. 323-349, 2004.
- [9] [S. Haykin, *Adaptive filter theory*, 2nd ed. NJ: Prentice-Hall, Englewood Cliffs, 1991.
- [10] S. Haykin, *Modern filters*. New York: Macmillan Publishing Company, 1989.
- [11] B. Widrow and E. Walach, *Adaptive inverse control*. New York: Prentice-Hall, Upper Saddle River, 1996.
- [12] P. A. Nelson, H. Hamada, and S. J. Elliott, "Adaptive inverse filters for stereophonic sound reproduction," *IEEE Transactions on Signal Processing*, vol. 40, pp. 1621-1632, 1992.